Double-wavelet double-difference time-lapse waveform inversion

Xin Fu, Sergio Romahn, Kris Innanen

ABSTRACT

Time-lapse seismic data are widely used to monitor reservoir changes. And time-lapse waveform inversion is a valuable tool for seismic exploration. A popular time-lapse waveform inversion strategy is the double-difference time-lapse waveform inversion (DDWI) (inversion of the differential data starting from the reverted baseline model). It is an effective way to solve the problem that baseline and monitor inversions of time-lapse waveform inversion are easily at different convergences, and it results in coherent model error in time-lapse inversion. Nevertheless, the double-difference method (DDWI) demands an almost perfect repeatability between the two baseline and monitor surveys, which is the most challenging for DDWI. Specially, when sources wavelets for the two data sets are different, the results of DDWI are seriously impacted. To solve this problem, we propose a double-wavelet double-difference time-lapse waveform inversion method (DWDDWI). This works because the data difference caused by wavelet difference is eliminated. DWDDWI is developed based on the convolution relationship between the shot gather and Green's function. And its premise is that the wavelets for both baseline and monitor data sets are known. To test the feasibility of this mothed, a numerical example is used.

INTRODUCTION

With the increasing of exploration requirements, more powerful seismic inversion tool is needed. As a potential power to recover physical properties of subsurface rock, the full waveform inversion (FWI) is introduced to seismic exploration by Lailly and Bednar (1983) and Tarantola (1984). It is researched widely and developing fast (Virieux and Operto, 2009). Since FWI can produce inversions with a high resolution, it is helpful to estimate the parameter difference related to the subsurface property change from time-lapse data sets.

Generally, the time-lapse inversion is performed as two parts, the baseline model inversion and the monitor model inversion, then the time-lapse model raises from the difference of the two inversions. For the linear system time-lapse model can be inverted directly from data difference between baseline and monitor data. However, FWI is of high nonlinearity, the procedure of two inversions is needed in general, at least, a reasonable starting model for monitor model inversion is necessary. Conventionally, the baseline inversion and monitor inversion are standalone, which use the same initial model (Plessix et al., 2010). To reduce the expensive computation of performing whole FWI for twice, some researchers utilize the inverted baseline model as the initial model for monitor data inversion, this also provides a better initial model for the monitor inversion (Oldenborger et al., 2007; Miller et al., 2008; Routh and Anno, 2008; Routh et al., 2012). Unfortunately, neither the two strategies mentioned above cannot essentially remove the coherence time-lapse model error attributed to the different convergence degrees between twice inversions. To address this problem, Watanabe et al. (2004) propose differential waveform tomography in frequency

domain performed to a crosswell time-lapse data set. Onishi et al. (2009) apply a similar scheme. After that this method is developed as double-difference waveform inversion (DDWI) (Watanabe et al., 2004; Onishi et al., 2009; Zheng et al., 2011; Zhang and Huang, 2013; Routh et al., 2012; Asnaashari et al., 2011, 2012, 2013, 2015; Maharramov and Biondi, 2014; Denli and Huang, 2009; Yang et al., 2015a). Successful real-data examples of DDWI are given by Yang et al. (2014, 2016) who use well-repeated ocean-bottom-cable data sets.

Nevertheless, the double-difference method (DDWI) demands a mostly perfect repeatability between the two surveys (Asnaashari et al., 2015), which is the most challenging for it. Specially, when source wavelets for baseline and monitor data sets are different, the results of DDWI are seriously impacted (Yang et al., 2015a). To solve this problem, we propose a double-wavelet double-difference time-lapse waveform inversion mothed (DWDDWI). This works because the data difference caused by wavelet difference is eliminated. DWDDWI is developed based on the convolution relationship between the shot gather and Green's function. And its premise is that the wavelets for both baseline and monitor data sets are known. To test the feasibility of this mothed, a numerical example is used.

Full waveform inversion (FWI)

Full waveform inversion (FWI) as an iterative inversion mothed estimates subsurface parameters by matching synthetic data ($\mathbf{u}_{syn}(\mathbf{m})$) , a function of model parameter $\mathbf{m}$, with observed data. The most common way to accomplish this is minimizing the L2 norm of data residual $\delta\mathbf{u}$ ($\mathbf{u}_{syn}(\mathbf{m}) - \mathbf{u}_{obs}$):

$$E(\mathbf{m}) = \frac{1}{2}\delta\mathbf{u}^T\delta\mathbf{u}. \tag{1}$$

The misfit function $E(\mathbf{m})$ depends on the model parameter $\mathbf{m}$. Within the framework of Born approximation, the updated model $\mathbf{m}$ is seen as a sum of reference model $\mathbf{m}_0$ and model perturbation $\Delta\mathbf{m}$ during the iterative inversion process. Using Taylor expansion and ignoring things behind and including second order term, we obtain linearized formula:

$$E(\mathbf{m}) = E(\mathbf{m}_0) + \frac{\partial E(\mathbf{m}_0)}{\partial \mathbf{m}}\Delta\mathbf{m}. \tag{2}$$

Continuously, taking the derivative with respect to $\mathbf{m}$, we have:

$$\frac{\partial E(\mathbf{m})}{\partial \mathbf{m}} = \frac{\partial E(\mathbf{m}_0)}{\partial \mathbf{m}} + \frac{\partial^2 E(\mathbf{m}_0)}{\partial \mathbf{m}^2}\Delta\mathbf{m}. \tag{3}$$

Setting the derivative as zero to minimize the above objective function, and after easy algebraic operations, we obtain:

$$\Delta\mathbf{m} = -\mathbf{H}^{-1}\mathbf{g}, \tag{4}$$

where $\mathbf{H} = \dfrac{\partial^2 E(\mathbf{m}_0)}{\partial \mathbf{m}^2}$ and $\mathbf{g} = \dfrac{\partial E(\mathbf{m}_0)}{\partial \mathbf{m}}$ are Hessian matrix and Jacobian matrix, respectively. To avoid the expensive computation of inversion Hessian matrix, gradient-based methods use identical matrix $\mathbf{I}$ as an approximate substitution of $\mathbf{H}$, such as steepest-descent (SD) method and non-linear conjugate gradient (NCG) method (Mora, 1987; Tarantola, 1984; Crase et al., 1990; Hu et al., 2011). In this paper, we apply the SD method for

FWI, which helps to converge globally (Hu et al., 2011), and the corresponding model perturbation with step length can be expressed as:

$$\Delta \mathbf{m} = -\mu \mathbf{g}. \tag{5}$$

It is the negative direction of gradient and the step length μ is a constant to scale the gradient. In this paper, we use the well-control method to calibrate the gradient, in which a segment of well log is used to figure out the step length as a factor fixing phase misfit and scaling the gradient, for details please refer toMargrave et al. (2011b) or Romahn and Innanen (2017). Also, we precondition the gradient with deconvolution imaging condition to compensate the spherical spreading of seismic wave (Margrave et al., 2011a), which can achieve the similar effect to that of approximate inverse Hessian of Shin et al. (2001) but avoid the calculation of Hessian.

Furthermore, for an acoustic waveform inversion with constant density in this paper, when the model $\mathbf{m}$ represents slowness of the subsurface medium, the specified expression for the gradient $\mathbf{g}$ expressed as a function of location $g(\mathbf{x})$ in time domain is (Tarantola, 1984; Yang et al., 2015b):

$$g(\mathbf{x}) = \sum_{r=1}^{ng} \sum_{i=1}^{ns} \int_0^{t_{max}} dt \left[-2s(\mathbf{x}) \frac{\partial^2 u_{syn}(\mathbf{x}, t; \mathbf{x}_s)}{\partial t^2} \delta u(\mathbf{x}, t; \mathbf{x}_r) \right]. \tag{6}$$

where ng, ns is the number of receivers and shots, respectively; t_{max} is the maximum forward/back ward propagating time t of wavefield; $\mathbf{x}$, $\mathbf{x_s}$, $\mathbf{x_r}$ is the location matrix in the model place as a whole, the location matrix for sources, and the location matrix for receivers, respectively; and s is the model slowness as a function of location $\mathbf{x}$; $u_{syn}(\mathbf{x}, t; \mathbf{x}_s)$ is forward wavefield with the source wavelet used to active the shots at location $\mathbf{x}_s$, and $\delta u(\mathbf{x}, t; \mathbf{x}_r)$ is backward/time-reversal wavefield using the data residual at location $\mathbf{x}_r$ as the source. In this paper the forward and back propagation wavefields are produced by phase shift plus interpolation (PSPI) migration (Gazdag and Sguazzero, 1984; Margrave et al., 2011b).

Time-lapse inversion strategies

Scheme I, parallel difference method. The parallel difference method considers the baseline inversion and monitor inversion as two independent produces which use the same initial model. Then the time-lapse model can be obtained by making a subtraction between the inverted monitor and baseline models. The main advantage of this approach is the applicability to acquisition geometries that do not match between the two experiments. As the two inversions are performed independently, a drawback is the potential interpretation of inversion artifacts as a real time-lapse response.

Scheme II, sequential difference method. As the time-lapse response in data is often weak with regard to the full data complexity, the sequential difference method uses the inverted baseline model as a starting model for the monitor data inversion. This means that the baseline is recovered first, and subsequently the baseline model is used to invert the monitor model. As the time-lapse response is weak, the baseline model should be a

good candidate for a starting model and should prevent too many iterations in the second inversion.

Scheme III, double-difference time-lapse waveform inversion (DDWI). The first inversion for the baseline data is the same as the above two schemes. But in the second inversion for the monitor data, instead of minimizing the difference between the observed and synthetic monitor data, DDWI attempts to minimize the difference of the differential data between the two data sets, and the misfit function without any constraints for the second inversion is:

$$E_{DDWI} = \frac{1}{2}\|R_2 - S_2\|^2 = \frac{1}{2}\|(\mathbf{R}_{monitor} - \mathbf{S}_{monitor}) - (\mathbf{R}_{baseline} - \mathbf{S}_{baseline})\|^2, \quad (7)$$

where $\mathbf{R}_2 = \mathbf{S}_{baseline} + (\mathbf{R}_{monitor} - \mathbf{R}_{baseline})$ is composed data for the monitor model inversion; $\mathbf{R}_{baseline}$, $\mathbf{S}_{baseline}$, and $\mathbf{R}_{monitor}$ are baseline data, synthetic data of the inverted baseline model obtained at the first baseline inversion, and monitor data, respectively; $\mathbf{S}_2 = \mathbf{S}_{baseline} + (\mathbf{S}_{monitor} - \mathbf{S}_{baseline}) = \mathbf{S}_{monitor}$ is the corresponding forward modeling data of $\mathbf{R}_2$ or the synthetic data of the updating monitor model during the inversion processing. However, the DDWI method demands a almost perfect repeatability between the baseline and monitor surveys, which is the most challenging for it. Specially, for the case of the wavelets for two data sets are different, the results of DDWI are seriously impacted. In the nest section, we propose a double-wavelet double-difference time-lapse waveform inversion method (DWDDWI) to solve this problem.

Double-wavelet double-difference time-lapse waveform inversion (DWDDWI)

The reason why the high repeatability is requested is that DDWI needs the difference between monitor and baseline data sets to generate the composed data. When the perfect repeatability is reached, the data difference only contains the seismic response related to the change of underground parameters, which enables DDWI to focus on the target. Nevertheless, when the wavelets of baseline and monitor data are different, the difference of two data sets will come from both the wavelet contrast and the subsurface change. Generally, the subsurface change is weak, the little difference between the wavelets can easily submerge the effective information and cause heavy artifacts in the final inverted time-lapse model (Yang et al., 2015a). We also display this phenomenon in the numerical example below. To eliminate the data difference casued by the wavelet differnece, when the wavelets for the two data sets are different, we will construct a common wavelet for the baseline and monitor data.

The composed data for the second monitor model inversion is flowing:

$$\mathbf{R}_2 = \mathbf{S}_{baseline} + (\mathbf{R}_{monitor} - \mathbf{R}_{baseline}), \quad (8)$$

To intuitively show how the subsurface parameter change influences the data set, we use Green's function to express the above equation. A seismic data can be expressed as the convolution between the source wavelet and Green' function, then equation 8 can be rewritten as:

$$\mathbf{R}_2 = \mathbf{S}_{baseline} + (\mathbf{W}_{monitor} * \mathbf{G}_{monitor} - \mathbf{W}_{baseline} * \mathbf{G}_{baseline}), \quad (9)$$

where $\mathbf{W}_{monitor}$ and $\mathbf{W}_{baseline}$ is the source wavelet for monitor and baseline shot data, respectively; $\mathbf{G}_{monitor}$ and $\mathbf{G}_{baseline}$ is Green' function for monitor and baseline shot data, respectively; and $\mathbf{S}_{baseline}$ is synthetic data using the baseline source wavelet. When $\mathbf{W}_{monitor}$ and $\mathbf{W}_{baseline}$ are equal, the difference is only from $\mathbf{G}_{monitor} - \mathbf{G}_{baseline}$ which is irrelevant to the wavelet. But in the case that $\mathbf{W}_{monitor}$ and $\mathbf{W}_{baseline}$ are unequal, the difference is from $\mathbf{W}_{monitor} * \mathbf{G}_{monitor} - \mathbf{W}_{baseline} * \mathbf{G}_{baseline}$ which is relevant both to the wavelets and Green' functions representing the property of the subsurface.

For the situation of baseline and monitor wavelets are different, we reconstruct monitor data by performing the convolution between baseline wavelet and monitor data, and reconstruct monitor data by performing the convolution between monitor wavelet and baseline data, then the new composed data becomes:

$$\begin{aligned}\mathbf{R}'_2 &= \mathbf{S}'_{baseline} + (\mathbf{R}'_{monitor} - \mathbf{R}'_{baseline}) \\ &= \mathbf{S}'_{baseline} + (\mathbf{W}_{baseline} * \mathbf{R}_{monitor} - \mathbf{W}_{monitor} * \mathbf{R}_{baseline}),\end{aligned} \tag{10}$$

expressed with Green's function as:

$$\begin{aligned}\mathbf{R}'_2 &= \mathbf{S}'_{baseline} + (\mathbf{W}_{baseline} * \mathbf{W}_{monitor} * \mathbf{G}_{monitor} - \mathbf{W}_{monitor} * \mathbf{W}_{baseline} * \mathbf{G}_{baseline}) \\ &= \mathbf{S}'_{baseline} + (\mathbf{W} * \mathbf{G}_{monitor} - \mathbf{W} * \mathbf{G}_{baseline}),\end{aligned} \tag{11}$$

where $\mathbf{W} = \mathbf{W}_{baseline} * \mathbf{W}_{monitor} = \mathbf{W}_{monitor} * \mathbf{W}_{baseline}$ is the double wavelet which used to forward modeling data $\mathbf{S}'_{baseline}$ during the iterative wave inversion. After performing the reconstructions to baseline and monitor data sets, the new data sets are of the same wavelet $\mathbf{W}$, the data difference is from $\mathbf{G}_{monitor} - \mathbf{G}_{baseline}$ related to the subsurface change only.

Numerical example

In this section, we use an anticline model shown in Figure 1a-b to test DWDDWI method and compare with the other methods. In Figure 2a-g, we show single shot records of baseline and monitor data sets. Figure 2a-d show the baseline and monitor shots using Ricker wavelets with 10Hz or 8Hz dominant frequency before performing the reconstruction, and Figure 2e-g show the corresponding reconstructed shots from performing the convolution. To show the feasibility of DWDDWI on eliminating the data difference caused by the wavelet difference, in Figure 3a-f, we show the data differences between the shots in Figure 2a-g. Figure 3a is the difference between baseline data with 10Hz wavelet and itself, of course it is zero. But the difference between baseline data with 10Hz wavelet and with 8Hz wavelet in Figure 3b is not zero, all the difference is caused by wavelet difference. In Figure 3c, we can see that the difference of reconstructed baseline shots is almost zero, quite tiny values. It illustrates that the impact of wavelet difference is eliminated perfectly. And Figure 3d-f, respectively, show the difference between the baseline shot with 10Hz wavelet and the monitor shot with 10Hz wavelet, the difference between the baseline shot with 10Hz wavelet and the monitor shot with 8Hz wavelet, and the difference between the reconstructed baseline shot and the reconstructed monitor shot. Obviously, in Figure 3e, the useful information corresponding to the time-lapse model is submerged in the wavelet impact, and in Figure 3f, the difference of the reconstructed shots shows that the impact caused by the wavelet difference is eliminated totally.

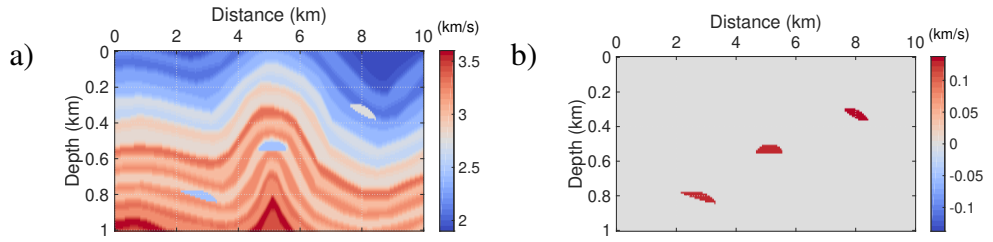

FIG. 1. (a) The true baseline model; (b) the true time-lapse model.

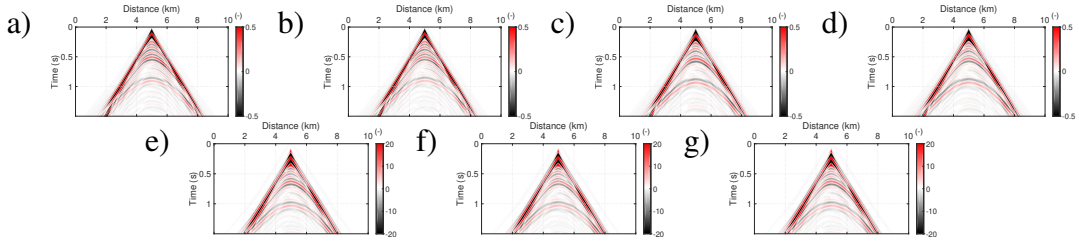

FIG. 2. (a) A single baseline shot with 10Hz wavelet; (b) a single monitor shot with 10Hz wavelet; (c) A single baseline shot with 8Hz wavelet; (d) a single monitor shot with 8Hz wavelet; (e) the reconstructed baseline shot of (a); (f) the reconstructed monitor shot of (b); (g) the reconstructed monitor shot of (c).

Next, we do the time-lapse inversions for all the three schemes. The initial model we use for the first baseline data inversion is shown in Figure 4a. And the inverted results of scheme I, II, and III are shown in Figure 4b-d. We can see that the coherence time-lapse model residual appears everywhere in the results of scheme I, II, but appears in a very small area in the result of scheme III (DDWI). In Figure 5a, we show the inverted time-lapse model of DDWI in the case of the baseline and monitor data is of 10Hz and 8Hz wavelet, respectively. Figure 5b is the inverted time-lapse model of DWDDWI in the case of the baseline and monitor data is of 10Hz and 8Hz wavelet, respectively. We can see that DDWI is seriously suffering from the unrepeatability of baseline and monitor data sets caused by wavelet difference, while DWDDWI can handle with this situation quiet well.

CONCLUSIONS

It is common view that the DDWI method has better difference recovery ability than the others. Compared with parallel difference and sequential difference time-lapse inversion strategies, DDWI is not easy to be affected by the different convergences between baseline and monitor data inversions. However, the DDWI method demands an almost perfect repeatability between baseline and monitor surveys, which is the most challenging for it. Specially, when source wavelets for baseline and monitor data sets are different, the results of DDWI are seriously impacted, but DWDDWI can handle with this situation well. DWDDWI works because the data difference caused by the wavelet difference is eliminated by the constructed common wavelet. DWDDWI is developed based on the convolution relationship between the shot gather and Green's function. And its premise is that the wavelets for both baseline and monitor data sets are known.

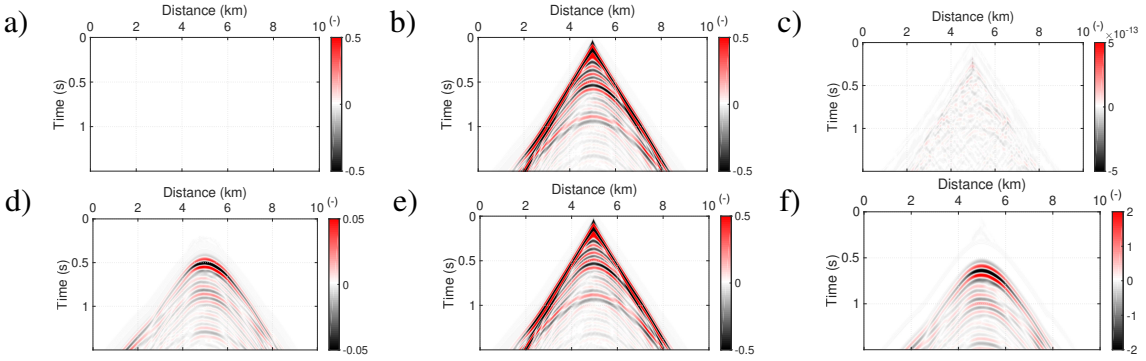

FIG. 3. (a) The difference between the baseline shot with 10Hz wavelet and itself; (b) the difference between baseline shots with 10Hz and 8Hz wavelets; (c) the difference between the reconstructed shot of the baseline shot with 10Hz wavelet and the reconstructed shot of the baseline shot with 8Hz wavelet; (d) the difference between the baseline shot with 10Hz wavelet and the monitor shot with 10Hz wavelet; (e) the difference between the baseline shot with 10Hz wavelet and the monitor shot with 8Hz wavelet; (f) the difference between the reconstructed shot of baseline shot with 10Hz wavelet and the reconstructed shot of the monitor shot with 8Hz wavelet.

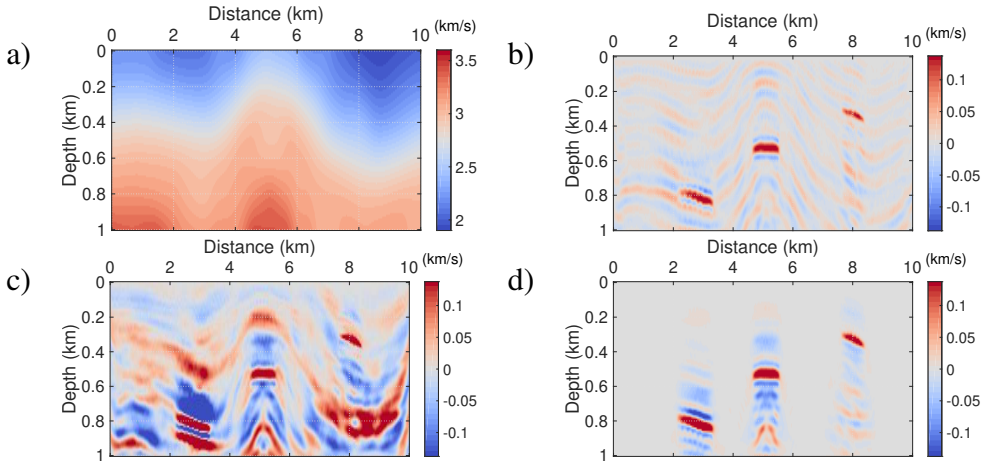

FIG. 4. (a) The initial baseline model; (b) the inverted time-lapse model of scheme I; (c) the inverted time-lapse model of scheme II; (d) the inverted time-lapse model of scheme III (DDWI).

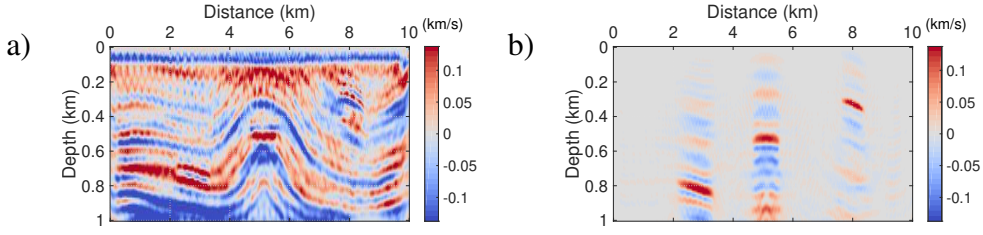

FIG. 5. (a) The inverted time-lapse model of DDWI when the source wavelet for the baseline data is 10Hz and the source wavelet for the monitor data is 8Hz; (b) the inverted time-lapse model of DWDDWI when the source wavelet for the baseline data is 10Hz and the source wavelet for the monitor data is 8Hz.

ACKNOWLEDGEMENTS

We thank the sponsors of CREWES for continued support. This work was funded by CREWES industrial sponsors, and NSERC (Natural Science and Engineering Research Council of Canada) through the grant CRDPJ 461179-13.

REFERENCES

Asnaashari, A., Brossier, R., Garambois, S., Audebert, F., Thore, P., and Virieux, J., 2011, Sensitivity analysis of time-lapse images obtained by differential waveform inversion with respect to reference model, *in* SEG Technical Program Expanded Abstracts 2011, Society of Exploration Geophysicists, 2482–2486.

Asnaashari, A., Brossier, R., Garambois, S., Audebert, F., Thore, P., and Virieux, J., 2012, Time-lapse imaging using regularized fwi: a robustness study, *in* SEG Technical Program Expanded Abstracts 2012, Society of Exploration Geophysicists, 1–5.

Asnaashari, A., Brossier, R., Garambois, S., Audebert, F., Thore, P., and Virieux, J., 2013, Regularized seismic full waveform inversion with prior model information: Geophysics, **78**, No. 2, R25–R36.

Asnaashari, A., Brossier, R., Garambois, S., Audebert, F., Thore, P., and Virieux, J., 2015, Time-lapse seismic imaging using regularized full-waveform inversion with a prior model: which strategy?: Geophysical prospecting, **63**, No. 1, 78–98.

Crase, E., Pica, A., Noble, M., McDonald, J., and Tarantola, A., 1990, Robust elastic nonlinear waveform inversion: Application to real data: Geophysics, **55**, No. 5, 527–538.

Denli, H., and Huang, L., 2009, Double-difference elastic waveform tomography in the time domain, *in* SEG Technical Program Expanded Abstracts 2009, Society of Exploration Geophysicists, 2302–2306.

Gazdag, J., and Sguazzero, P., 1984, Migration of seismic data by phase shift plus interpolation: Geophysics, **49**, No. 2, 124–131.

Hu, W., Abubakar, A., Habashy, T., and Liu, J., 2011, Preconditioned non-linear conjugate gradient method for frequency domain full-waveform seismic inversion: Geophysical Prospecting, **59**, No. 3, 477–491.

Lailly, P., and Bednar, J., 1983, The seismic inverse problem as a sequence of before stack migrations, *in* Conference on inverse scattering: theory and application, Siam Philadelphia, PA, 206–220.

Maharramov, M., and Biondi, B., 2014, Joint full-waveform inversion of time-lapse seismic data sets, *in* SEG Technical Program Expanded Abstracts 2014, Society of Exploration Geophysicists, 954–959.

Margrave, G., Yedlin, M., and Innanen, K., 2011a, Full waveform inversion and the inverse hessian: the 23rd Annual Research Report of the CREWES Project.

Margrave, G. F., Ferguson, R. J., and Hogan, C. M., 2011b, Full waveform inversion using wave-equation depth migration with tying to wells, *in* SEG Technical Program Expanded Abstracts 2011, Society of Exploration Geophysicists, 2454–2458.

Miller, C. R., Routh, P. S., Brosten, T. R., and McNamara, J. P., 2008, Application of time-lapse ert imaging to watershed characterization: Geophysics, **73**, No. 3, G7–G17.

Mora, P., 1987, Nonlinear two-dimensional elastic inversion of multioffset seismic data: Geophysics, **52**, No. 9, 1211–1228.

Oldenborger, G. A., Routh, P. S., and Knoll, M. D., 2007, Model reliability for 3d electrical resistivity tomography: Application of the volume of investigation index to a time-lapse monitoring experiment: Geophysics, **72**, No. 4, F167–F175.

Onishi, K., Ueyama, T., Matsuoka, T., Nobuoka, D., Saito, H., Azuma, H., and Xue, Z., 2009, Application of crosswell seismic tomography using difference analysis with data normalization to monitor co2 flooding in an aquifer: International Journal of Greenhouse Gas Control, **3**, No. 3, 311–321.

Plessix, R.-E., Michelet, S., Rynja, H., Kuehl, H., Perkins, C., de Maag, J., and Hatchell, P., 2010, Some 3d applications of full waveform inversion, *in* 72nd EAGE Conference and Exhibition-Workshops and Fieldtrips.

Romahn, S., and Innanen, K. A., 2017, Iterative modeling, migration, and inversion: Evaluating the well-calibration technique to scale the gradient in the full-waveform inversion process, *in* SEG Technical Program Expanded Abstracts 2017, Society of Exploration Geophysicists, 1583–1587.

Routh, P., Palacharla, G., Chikichev, I., and Lazaratos, S., 2012, Full wavefield inversion of time-lapse data for improved imaging and reservoir characterization, *in* SEG Technical Program Expanded Abstracts 2012, Society of Exploration Geophysicists, 1–6.

Routh, P. S., and Anno, P. D., 2008, Time-lapse noise characterization by inversion, *in* SEG Technical Program Expanded Abstracts 2008, Society of Exploration Geophysicists, 3143–3147.

Tarantola, A., 1984, Inversion of seismic reflection data in the acoustic approximation: Geophysics, **49**, No. 8, 1259–1266.

Virieux, J., and Operto, S., 2009, An overview of full-waveform inversion in exploration geophysics: Geophysics, **74**, No. 6, WCC1–WCC26.

Watanabe, T., Shimizu, S., Asakawa, E., and Matsuoka, T., 2004, Differential waveform tomography for time-lapse crosswell seismic data with application to gas hydrate production monitoring, *in* SEG Technical Program Expanded Abstracts 2004, Society of Exploration Geophysicists, 2323–2326.

Yang, D., Liu, F., Morton, S., Malcolm, A., and Fehler, M., 2016, Time-lapse full-waveform inversion with ocean-bottom-cable data: Application on valhall field: Geophysics, **81**, No. 4, R225–R235.

Yang, D., Malcolm, A., and Fehler, M., 2014, Time-lapse full waveform inversion and uncertainty analysis with different survey geometries, *in* 76th EAGE Conference and Exhibition 2014.

Yang, D., Meadows, M., Inderwiesen, P., Landa, J., Malcolm, A., and Fehler, M., 2015a, Double-difference waveform inversion: Feasibility and robustness study with pressure data: Geophysics, **80**, No. 6, M129–M141.

Yang, P., Gao, J., and Wang, B., 2015b, A graphics processing unit implementation of time-domain full-waveform inversion: Geophysics, **80**, No. 3, F31–F39.

Zhang, Z., and Huang, L., 2013, Double-difference elastic-waveform inversion with prior information for time-lapse monitoring: Geophysics, **78**, No. 6, R259–R273.

Zheng, Y., Barton, P., and Singh, S., 2011, Strategies for elastic full waveform inversion of time-lapse ocean bottom cable (obc) seismic data, *in* SEG Technical Program Expanded Abstracts 2011, Society of Exploration Geophysicists, 4195–4200.